

A milestone in ribosomal crystallography: the construction of preliminary electron density maps at intermediate resolution

F. Schlünzen, H.A.S. Hansen, J. Thygesen, W.S. Bennett, N. Volkmann, I. Levin, J. Harms, H. Bartels, A. Zaytzev-Bashan, Z. Berkovitch-Yellin, I. Sagi, F. Franceschi, S. Krumbholz, M. Geva, S. Weinstein, I. Agmon, N. Böddeker, S. Morlang, R. Sharon, A. Dribin, E. Maltz, M. Peretz, V. Weinrich, and A. Yonath

Abstract: Preliminary electron density maps of the large and the small ribosomal particles from halophilic and thermophilic sources, phased by the isomorphous replacement method, have been constructed at intermediate resolution. These maps contain features comparable in size with what is expected for the corresponding particles, and their packing arrangements are in accord with the schemes obtained by ab-initio procedures as well as with the motifs observed in thin sections of the crystals by electron microscopy. To phase higher resolution data, procedures are being developed for derivatization by specific labeling of the ribosomal particles at selected locations with rather small and dense clusters. Potential binding sites are being inserted either by site directed mutagenesis or by chemical modifications to facilitate cluster binding on the surface of the halophilic large and the thermophilic small ribosomal particles, which yield the crystals diffracting to highest resolution (2.9 and 7.3 Å (1 Å = 0.1 nm), respectively). For this purpose, the surface of these ribosomal particles is being characterized and procedures are being developed for quantitative detachment of selected ribosomal proteins and for their incorporation into core particles. The genes of these proteins are being cloned, sequenced, mutated to introduce reactive side groups, mainly cysteines, and overexpressed. In parallel, two in situ small and stable complexes were isolated from the halophilic ribosome. Procedures for their crystal production in large quantities are currently being developed. Models, reconstructed at low resolution from crystalline arrays of ribosomes and their large subunits, are being used for initial low-resolution phasing of the X-ray amplitudes. The interpretation of these models stimulated the design and the crystallization of complexes mimicking defined functional states of a higher quality than those obtained for isolated ribosomes. These models also inspired modelling experiments according to results of functional studies, performed elsewhere, focusing on the progression of nascent proteins.

Key words: ribosomes, crystallography, undecagold cluster, heteropolyanions.

Received May 20, 1995. Accepted August 10, 1995.

Abbreviations: 70S, 30S, and 50S, the commonly used names for bacterial ribosomes and their small and large subunits, respectively, given according to their sedimentation coefficients; E, B, T, and H in front of these names or the number of a ribosomal protein show the bacterial source (*Escherichia coli*, *Bacillus stearothermophilus*, *Thermus Thermophilus*, and *Haloarcula marismortui*, respectively); rRNA and r-proteins, ribosomal RNA and ribosomal proteins; for proteins, L shows that the protein is of the large (50S) subunit, and S of the small (30S) one (e.g., BL11 is protein 11 in the large ribosomal subunit from *B. stearothermophilus*); the symbol HmaL# indicates that this particular protein (of *H. marismortui*) is homologous to protein # from *E. coli*; MIR, SIR: the multiple and single isomorphous-phasing methods.

F. Schlünzen, H.A.S. Hansen, J. Thygesen, W.S. Bennett, N. Volkmann, J. Harms, H. Bartels, and S. Krumbholz. Max-Planck Laboratory for Ribosomal Structure, Hamburg, Germany.

I. Levin, A. Zaytzev-Bashan, M. Geva, S. Weinstein, I. Agmon, R. Sharon, A. Dribin, E. Maltz, M. Peretz, and V. Weinrich. Department of Structural Biology, Weizmann Institute, Rehovot, Israel.

F. Franceschi, N. Böddeker, and S. Morlang. Max-Planck Institute for Molecular Genetics, Berlin, Germany.

Z. Berkovitch-Yellin and A. Yonath.¹ Max-Planck Laboratory for Ribosomal Structure, Hamburg, Germany, and Department of Structural Biology, Weizmann Institute, Rehovot, Israel.

I. Sagi. Max-Planck Laboratory for Ribosomal Structure, Hamburg, Germany, and Max-Planck Institute for Molecular Genetics, Berlin, Germany.

¹ Author to whom all correspondence should be addressed at Max-Planck Laboratory for Ribosomal Structure, c/o DESY/Notkestr. 85, 22603 Hamburg, Germany.

Résumé : Des cartes de densité électronique préliminaires de la petite et de la grande sous-unités ribosomiques de bactéries halophiles et thermophiles, mises en phase par la méthode de substitution isomorphe, ont été construites à résolution intermédiaire. Ces cartes contiennent des caractéristiques comparables à celles prédites pour les sous-unités correspondantes, et leur agencement est en accord avec les modèles établis par des méthodes partant du début et avec les motifs observés dans des coupes minces des cristaux par microscopie électronique. Afin de mettre en phase des données à plus haute résolution, des méthodes de dérivation ont été mises au point en marquant les sous-unités ribosomiques à des endroits spécifiques avec des groupes plutôt petits et denses. Afin de faciliter la liaison des groupes à la surface de la grande sous-unité ribosomique halophile et de la petite sous-unité ribosomique thermophile, ce qui donne des cristaux diffractant à la plus haute résolution (respectivement à 2,9 et 7,3 Å (1 Å = 0,1 nm)), des sites de liaison potentiels sont insérés par mutagenèse dirigée ou par modification chimique. Actuellement, la surface de ces sous-unités ribosomiques est caractérisée, des méthodes sont mises au point pour la libération de protéines ribosomiques spécifiques de façon quantitative et pour leur incorporation dans des sous-unités. Les gènes de ces protéines sont clonés, séquencés, mutés afin d'introduire des résidus ayant un groupe réactif, principalement des cystéines, et surexprimés. En parallèle, deux petits complexes stables in situ ont été isolés des ribosomes halophiles. En vue de leur cristallisation, des méthodes pour les produire en grande quantité sont mises au point. Des modèles, reconstruits à faible résolution à partir de la structure cristalline des ribosomes et de leurs grandes sous-unités, sont utilisés pour la mise en phase initiale à faible résolution de l'amplitude des rayons X. L'interprétation de ces modèles a stimulé la conception et la cristallisation de complexes imitant des états fonctionnels définis, d'une plus grande qualité que celle obtenue avec des ribosomes isolés. Ces modèles ont également suscité des expériences de modélisation de la progression des protéines naissantes basées sur les résultats d'études fonctionnelles réalisées dans d'autres laboratoires.

Mots clés : ribosomes, cristallographie, groupe à onze atomes d'or, hétéropolyanions.

[Traduit par la rédaction]

Introduction

To shed light on the molecular mechanisms involved in protein biosynthesis, crystallographic analysis of the three-dimensional structure of the ribosome is being carried out using crystals of intact ribosomal particles from halophilic and thermophilic bacteria, which diffract best to 2.9 Å (1 Å = 0.1 nm) resolution (of the large ribosomal subunits of *H. marismortui*, von Böhlen et al. 1991). The crystallized systems include 70S ribosomes and their complexes mimicking defined functional states, as well as natural, modified, and mutated ribosomal subunits (Berkovitch-Yellin et al. 1992). Crystallographic data are being collected at cryo temperature from shock-frozen crystals with bright synchrotron radiation. As a result of continuous refinement of the crystal growth conditions and the data collection instrumentation and parameters, the crystallographic data collected from these crystals are of reasonable quality, which in many cases is comparable with the data obtained from crystalline proteins of average size.

In this manuscript, we present an overview of our structural efforts, highlighting the construction of the first electron density maps for the small and the large subunits, obtained by experimental crystallographic methods and supported by ab-initio procedures. We also describe our plans for the construction of electron density maps for the ribosome and its functional complexes and for extending the level of detail of the current maps. The various strategies expected to be taken for the interpretation of the maps are also being discussed.

Assignment of phases in ribosomal crystallography

The assignment of phases to the observed structure factor amplitudes is the most crucial, albeit most complicated and

unpredictable, step in structure determination, even for average-sized proteins of molecular weights of 15 000 – 80 000. Clearly, for ribosomal crystals, the magnitude and the complexity of this step are greatly enhanced. Therefore, a multidirectional algorithm has been designed using the commonly used phasing techniques, namely those based on isomorphous replacement, side by side with efforts at very low resolution phasing by pure computational and semiexperimental procedures.

Low-resolution phase information obtained by computational approaches

In small molecule crystallography, phases are routinely obtained by ab-initio methods (Giacovazzo 1980). Obviously, a considerable effort has been devoted to the extension of these methods towards macromolecules, and a large range of approaches is being exploited in the context of low-resolution phasing of the ribosomal reflections.

Entropy maximization with log likelihood gain as a phase-set discriminator (Bricogne 1984) was used to suggest the packing and to detect some envelope features of T50S at a resolution of about 80 Å (Volkman 1993, 1995). These results were later supported by the application of the few atom method (Lunin et al. 1995) and by low-resolution molecular replacement studies (Urzhumtsev and Podjarny 1995), using the approximate model reconstructed for this particle (Yonath et al. 1987). Molecular replacement studies with this model have also been performed on other crystal forms (Berkovitch-Yellin et al. 1990; Eisenstein et al. 1991).

Furthermore, the positioning of the center of mass of T50S was supported by results of ultra-low-resolution R-factor searches at various solvent contrasts (Volkman 1993; Schlünzen 1994) and by the application of an extension of traditional direct methods combined with ellipsoidal modelling (Roth and Pebay-Peyroula 1995; Zaytzev-Bashan 1995).

Table 1. Heavy atom compounds used for soaking.

TAMM*
$(\text{NH}_4)_6(\text{P}_2\text{W}_{18}\text{O}_{62})14\text{H}_2\text{O}$
$\text{K}_{14}\text{NaP}_5\text{W}_{30}\text{O}_{110}$
$(\text{K}_5\text{O}_2)_3(\text{PW}_{12}\text{O}_{40})$
$\text{Na}_{16}((\text{O}_3\text{PCH}_2\text{PO}_3)_4\text{W}_{12}\text{O}_{36})_n\text{H}_2\text{O}$
$\text{Cs}_7(\text{P}_2\text{W}_{17}\text{O}_{61}\text{Co}(\text{NC}_5\text{H}_5))_n\text{H}_2\text{O}$
$\text{K}_5\text{H}_4((\text{phSn})_3(\text{P}_2\text{W}_{15}\text{O}_{59}))_n\text{H}_2\text{O}$ (ph = phenyl)
$\text{K}_5\text{H}_4((\text{buSn})_3(\text{P}_2\text{W}_{15}\text{O}_{59}))_n\text{H}_2\text{O}$ (bu = butyl)
$\text{K}_7((\text{buSn})_3(\text{P}_2\text{W}_{17}\text{O}_{61}))_n\text{H}_2\text{O}$
$\text{K}_{11}\text{H}((\text{buSnOH})_3(\text{PW}_9\text{O}_{34}))_n\text{H}_2\text{O}$
$\text{K}_4\text{H}_3((\text{buSn})_3(\text{alfaSiW}_9\text{O}_{31}))_2)_n\text{H}_2\text{O}$
$\text{Cs}_9\text{H}_6((\text{buSnO})_3(\text{alfaSiW}_9\text{O}_{31}))_2)_n\text{H}_2\text{O}$
$\text{Ta}_6\text{Br}_{12}\cdot\text{Cl}_2\cdot 8\text{H}_2\text{O}$
$\text{Ta}_6\text{Br}_{14}\cdot 8\text{H}_2\text{O}$

*TAMM, tetrakis(acetoxymethyl)mercuric methane.

A new approach, combining elements of traditional direct methods, envelope refinement, maximum entropy filtering, likelihood ranking, cross validation and cluster analysis, aimed at phasing at resolution of up to 30 Å (N. Volkman, to be published) has been applied to T50S and led to results that agree well with the previous ones (Volkman et al. 1995). The same approach was applied to data from H50S crystals, and the resulting weights and phases were used to locate heavy atom sites by difference Fourier calculations (N. Volkman and H.A.S. Hansen, to be published), which were found to be the same as determined by difference Patterson interpretation (see below).

Direct information about packing motifs of the ribosomal crystals has been derived by electron microscopy since the large size of the ribosome enables its observation. In these experiments, three-dimensional crystals are embedded in epon and sectioned at preferred orientations to extremely thin slices of a thickness similar to one unit cell. Optical diffraction information, obtained from their electron micrographs, together with visual inspection and symmetry considerations can be exploited to yield information about the packing arrangements of the crystals. This information was combined with the results of real and reciprocal space searches and led to the determination of the number of the ribosomal particles in the asymmetric unit (see below and Bartels et al. 1995).

First steps in the application of the isomorphous replacement method

The commonly used method for the determination of the phases of unknown structures of macromolecules is the isomorphous replacement. It is based on the changes in the structure factor amplitudes caused by the addition of heavy atoms to the native crystals. Successful derivatization requires attachment of heavy atoms at a limited number of sites within the unit cell while keeping the crystal structure isomorphous to that of the native molecule. When only one derivative is available, the single isomorphous replacement (SIR) procedure, which yields ambiguous phasing, is used. When more than one such derivative can be obtained, MIR (multiple isomorphous replacement) is used.

Because the differences in the intensities of the reflections of the native and derivatized crystals are used for phasing, the added compounds are chosen according to their potential ability to induce measurable signals. Useful heavy atom derivatives for proteins of average size consist of one or two heavy-metal atoms. Because of the large size of the ribosome, ideal compounds for derivatization are compact and dense materials of a proportionally larger number of electrons. Multi-metal salts, such as polyheteroanions and coordination compounds (Table 1), or dense metal clusters, such as undecagold (Jahn 1989a), have been shown to be of adequate phasing power by simulation studies (Bartels et al. 1995).

The derivatization of macromolecular crystals may be performed in two ways: (i) by soaking crystals in solutions containing the heavy atoms or (ii) by covalent specific binding of the heavy atom before crystallization. Soaking is the more common way since the experimental requirements are rather simple and the results can be assessed in a relatively short time. Using this trial-and-error procedure, productive single-site derivatization is largely a matter of chance, but the probabilities of successful derivatization are sufficiently high that more sophisticated techniques are rarely needed.

Preliminary phasing at 19 Å resolution of X-ray data of T30S
Soaking crystals of T30S (Yonath et al. 1988) in solutions containing the heteropolyanion $(\text{NH}_4)_6(\text{P}_2\text{W}_{18}\text{O}_{62})14\text{H}_2\text{O}$ (Dawson 1953) or $(\text{K}_5\text{O}_2)_3(\text{PW}_{12}\text{O}_{40})$ (Brown et al. 1977) led to preliminary phasing at 15 Å resolution. A third derivative, $\text{Ta}_6\text{Br}_{14}$, which proved to be useful for structure determination of large assemblies and proteins (Schneider and Lindquist 1994; Löwe et al. 1995), is currently being investigated.

Initially, the two W derivatives were phased independently, using only the centric reflection for the construction of two SIR maps at about 20 Å resolution. No attempt was made to resolve the individual atoms of the heteropolyanions, which were treated as group scatterers. The 12 W atoms cluster was approximated to a sphere, whereas the 18 W atoms cluster, which has an ellipsoidal shape and is actually composed of two 9 W atoms clusters, was represented by two 9 W scatterers. The figures of merit of these maps are 0.57 for 240 centric reflections (phasing power 1.78) and 0.44 for 270 centric reflections (phasing power 1.02). More details about the data are given in Table 2.

Combining the phase information from both derivatives yielded an uninterpretable 19 Å MIR electron density map. However, after several cycles of solvent flattening combined with density modification, the resulting electron density map (Fig. 1) contains features that may be interpreted as small ribosomal particles, and its packing motif is in agreement with that observed in thin sections of embedded crystals (Fig. 1). Furthermore, this map shows striking agreement with that constructed from independent phase information (Fig. 1) obtained by the maximum entropy combined by likelihood ranking approach (Volkman et al. 1995).

Despite the reasonable quality of the crystallographic parameters of the preliminary MIR map, the borders of the individual particles are still not clear. Attempts towards this aim are currently being carried out, and the map is subjected to phase extension to considerably higher resolution, 12–14 Å.

Table 2. Medium resolution phasing of T30S.

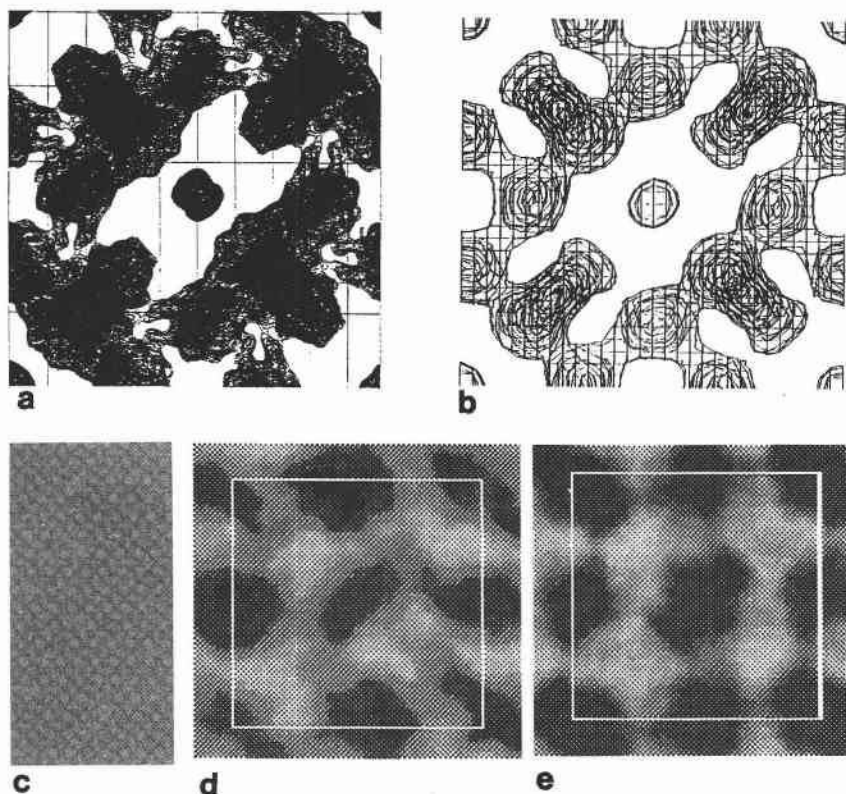
	Native	Wo(12)	Wo(18)	Ta ₆ Br ₁₄
Resolution, Å	290–15	83–12	50–15	98–10
R_{merge}	0.077	0.075	0.087	0.078
Completeness, %	64	60	60	74
R_{deriv}		0.35	0.42	0.22
No. of major sites*		3 (5)	2	—
$R_{\text{cullis}}^{\dagger}$		0.83(0.76)	0.76(0.65)	—
Phasing power [†]		1.61(1.22)	1.9(1.78)	—

Note: Space group, P4₂2. Unit cell: 407, 407, 169.

*Numbers in parentheses are possible extra sites.

†Numbers in parentheses are for centric reflections.

Fig. 1. The current preliminary electron density maps of T30S. (a) The MIR map at 19 Å resolution after several cycles of solvent flattening assuming 66% solvent, with final figures of merit of 0.59 and 0.38 for the centric and acentric reflections, respectively. The whole unit cell is shown, down the *c* axis. The crystals were soaked for 43 and 14 h in solutions of 3 mM of (NH₄)₆(P₂W₁₈O₆₂)14H₂O and (K₅O₂)₃(PW₁₂O₄₀), respectively. Two major sites were located for the first derivative, and five for the second. The latter were partially located in the difference Patterson map and partially in difference Fourier, exploiting the phase information obtained by the first derivative. The combined Fourier figure of merit is 0.67. (b) The 40–50 Å map constructed with the amplitudes used in *a* and *ab initio* phases. (c) A positively stained thin section of embedded T30S crystal. (d) Comparison between the observed filtered image of *c* (d) and the simulated packing arrangement, based on the *ab initio* phases (e).



Preliminary phasing at 7 Å resolution of X-ray data of H50S
 Preliminary partial phase information was obtained for the crystals of H50S (von Böhlen et al. 1991) by soaking crystals in solutions of K₁₄NaP₅W₃₀O₁₁₀ (Alizadeh et al. 1985),

(NH₄)₆(P₂W₁₈O₆₂)14H₂O (Dawson 1953), (K₅O₂)₃-(PW₁₂O₄₀) (Brown et al. 1977), and Cs₇(P₂W₁₇O₆₁-Co(NC₅H₅))nH₂O (M. Pope, private communication). Although the resolution of the soaked crystals was lower than

Table 3. Medium resolution phasing of H50S.

	Native	Wo(30)	Wo(18)	K-Wo(12)	Co-Wo(17)
Resolution (used), Å	5.2	12.0	7.0	9.0	9.0
R_{merge}	0.084	0.101	0.124	0.095	0.103
Completeness, %	74.4	78	91	70	78
R_{deriv}		0.25	0.15	0.30	0.19
No. of major sites*		2 (4)	2 (4)	1 (2)	4 (5)
$R_{\text{cutis}}^{\dagger}$		0.80(0.70)	0.89(0.89)	0.75(0.88)	0.90(0.90)
Phasing power ‡		1.36(0.88)	0.8(0.52)	1.39(0.9)	0.70(0.43)

Note: Space group, C222₁. Unit cell: 212, 302, 567.

*Numbers in parentheses are possible extra sites.

‡ Numbers in parentheses are for centric reflections.

that of the native ones (2.9 Å), all derivatives diffracted well beyond 7 Å, and in many cases, well-shaped reflections were detected at 3.5–5 Å. However, because of technical reasons and synchrotron beam-time limitations, data were collected only to lower resolution. The initial difference Patterson map was constructed at 12 Å resolution, using the data collected from a crystal soaked in K₁₄NaP₅W₃₀O₁₁₀. Significant sophistication was required for the interpretation of the difference Patterson maps, including partial assignment of the individual atoms. Nevertheless, the sites detected in the difference Patterson map were reconfirmed by ab-initio calculations (see above). More details about the data are given in Table 3.

These phases were used for the construction of the difference electron density maps between the native and the other three derivatives, which revealed that all four clusters occupy roughly the same site. Therefore, their phase information was used mainly for extending the resolution of the initial map. The connectivity within the map was significantly enhanced when the lower resolution reflections were included, and it was subjected to two cycles of solvent flattening, assuming that the crystals contain 65% solvent (Fig. 2).

Phasing at 26 Å of X-ray data of B50S by covalent labeling with an undecagold cluster

A SIR electron density map of B50S (Müssig et al. 1989) was obtained at 26 Å resolution using a heavy atom derivative formed by specific quantitative derivatization with a dense undecagold cluster (Bartels et al. 1995). This approach was chosen, although it requires sophisticated synthetic techniques and time-consuming purification procedures, because it maximizes the chances of obtaining a unique derivative with full occupancy.

A monofunctional reagent was prepared from an undecagold cluster composed of a core of densely packed Au atoms linked directly to each other (Jahn 1989a). The core of the undecagold cluster is about 8.2 Å in diameter (Jahn 1989a) and, therefore, can be treated as a single scattering group at low to medium resolution. For testing the phasing power of the undecagold cluster, our biochemically favorable albeit crystallographically weakest, particles, B50S, were chosen, although their crystals are unstable, packed with a very low symmetry, and diffract to low resolution (Müssig et al. 1989), because their biochemistry and genetics are rather well characterized. These particles possess an exposed –SH group on a

Fig. 2. The current electron density map of H50S. The MIR map at 7 Å resolution after several cycles of solvent flattening assuming 65% solvent. A projection of half a unit cell is shown, down the *a* axis. The crystals were soaked for up to 34 days in solutions containing 1–2 mM of the following clusters: K₁₄NaP₅W₃₀O₁₁₀, (NH₄)₆(P₂W₁₈O₆₂)14H₂O, (K₅O₂)₃(PW₁₂O₄₀), and Cs₇(P₂W₁₇O₆₁Co(NC₅H₅))_nH₂O. For all sets the $R_{\text{merge}}(I) = 8.4$ –10.3% and the completeness is 74–91%. Two major sites were located for the first two derivatives, one for the third, and four for the fourth, with occupancies between 0.2 and 0.6. Phasing power was between 0.7 (for the W₁₇Co cluster) and 1.36 (for the W₃₀ cluster). The overall figure of merit, after two cycles of solvent flattening (assuming 65% solvent), is around 0.65.

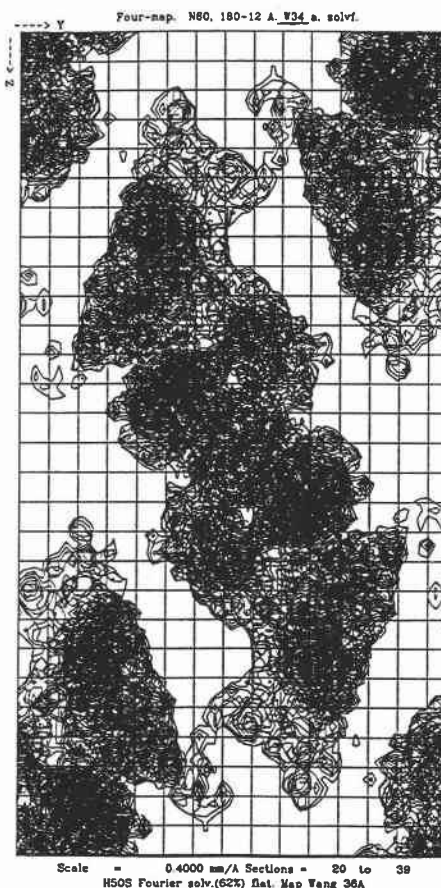
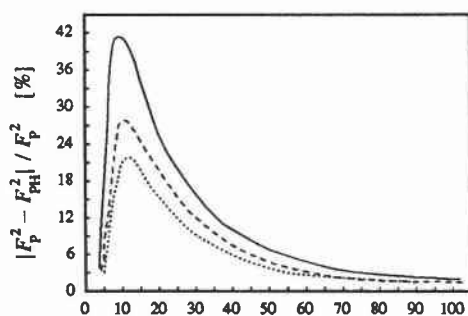
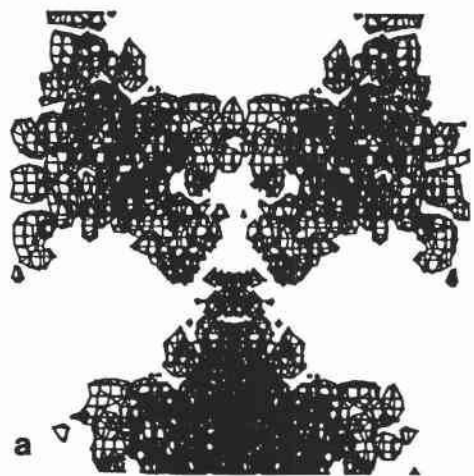


Fig. 3. (a) The electron density map of B50S after two cycles of solvent flattening, assuming 61% solvent, combined with phase combination. The whole unit cell, down the z direction, is shown. Resolution range, 26–60 Å, figure of merit, 0.71 (Bartels et al. 1995). (b) Simulation of the expected changes in the intensity by the addition of an undecagold cluster to 30S (solid lines), 50S (broken), and 70S particles (dotted). The structure factor intensities of ribosomal particles and the undecagold cluster were calculated based on their molecular composition. Full occupancy of the cluster was assumed and the mean displacement of the cluster position was restricted to 1 Å.



b Resolution [Å]

protein that is readily detached from the ribosome (BL11) and a mutant, lacking this protein, could be obtained by the addition of the antibiotic thiostrepton to the bacterial growth medium.

The monofunctional reagent of the undecagold cluster was bound to isolated protein BL11, exploiting its only cysteine. Remarkably, although the binding of the cluster was carried out under denaturing conditions and the molecular mass of the undecagold cluster (6200 Da) approaches half of that of the protein (15 500 Da), the cluster-bound protein was incorporated into cores lacking this protein, yielding fully derivatized particles. Because of the significant lack of isomorphism and the nonuniform mosaic spread, a few data sets had to be collected before a sufficiently isomorphous couple was detected.

Some of these sets contain reflections to 11 to 15 Å resolution; however, meaningful differences were obtained only at lower resolution. After resolving the SIR phase ambiguity by solvent flattening, the resulting 26 Å electron density map (Fig. 3) shows packing arrangement of symmetry consistent with the noncrystallographic symmetry found by the self-rotation function as well as with the motif observed in electron micrographs of thin sections of these crystals.

The extension of the procedures for specific labeling to halophilic and thermophilic ribosomes

Specific derivatization at predetermined sites on selected ribosomal components may have a considerable value not only in phasing the crystallographic data but also in the localization of the sites to which the heavy atoms are bound. Such information may be indispensable for the interpretation of high resolution electron density maps. The studies performed with the undecagold cluster established that phase information can be obtained from bound heavy-metal clusters, even when the crystals under investigation are unstable and weakly diffracting, and encouraged further effort at the construction of specifically derivatized crystals from the ribosomal particles that diffract to higher resolution, namely H50S and T30S. Assuming that the preliminary intermediate resolution electron density maps, whose phases were obtained by soaking, are approximately right, the labeling with the large undecagold cluster is being extended to the binding of smaller dense clusters, such as TAMM (Table 1) or a tetrairidium cluster (Jahn 1989b). As these clusters are significantly lighter than the undecagold cluster, for obtaining measurable signals, procedures are being developed for their binding in multiple sites.

It was soon found that a straightforward extension of the procedures developed for B50S to H50S and T30S was not possible because there are no naturally exposed sulfhydryls on the surfaces of these particles suitable for derivatization with the undecagold cluster. In addition, because of the significant resistance of the halophilic ribosomes to mutagenesis, no protein-depleted core particles could be produced by growing the bacteria on medium containing antibiotics. Also, the chemical methods used for quantitative detachment of selected *E. coli* ribosomal proteins were found unsuitable for the halophilic systems. Furthermore, in contrast with the ease of the incorporation of the gold cluster bound protein BL11 into depleted cores of *B. stearothermophilus*, protein HmaL11, the halophilic homolog of BL11 (Franceschi et al. 1993), can be reconstituted into core H50S particles only when its sulfhydryl group is free.

Consequently, the potential heavy-atom binding sites on the surfaces of the halophilic ribosomes are being either created by chemical modifications or inserted by genetic procedures (Franceschi et al. 1994; Sagi et al. 1995). For choosing appropriate locations for these insertions, procedures for specific quantitative detachment and reconstitution of selected ribosomal proteins are being developed, and the surfaces of these ribosomal particles are being mapped chemically and enzymatically. Sequence information is essential for the surface mapping experiments as well as for the insertion of the binding sites. To date, over one-third of the ribosomal proteins from *T. thermophilus* (e.g., Tsuboli et al. 1994) and more than

two-thirds of those from *H. marismortui* have been fully or partially sequenced (Wittmann-Liebold et al. 1990; Franceschi et al. 1996).

Selective detachment and reconstitution of ribosomal proteins, surface characterization, and side chain modifications

Procedures were developed under which six ribosomal proteins (S2, S3, S5, S9, S10, and S14) can be fully detached from T30S (3.4 M LiCl and 0.5 M urea for 2 h at 4°C, with gentle agitation, Franceschi et al. 1996). All detached proteins could be reconstituted into the cores lacking them, and the resulting reconstituted particles showed 60% of the original poly(Phe) synthesizing activity.

In parallel experiments, two ribosomal proteins were removed quantitatively by dioxane from H30S. Both detached proteins could be fully reconstituted into the depleted core particles (Franceschi et al. 1996). Using the same procedure, cores of H50S particles, depleted of four proteins, HmaL1, HmaL10, HmaL11, and HmaL12, were prepared. All detached proteins can be fully reconstituted and the resulting particles crystallized under the same conditions as native H50S subunits. However, blocking the -SH group of one of the proteins, HmaL11, prevented its incorporation into the core particles. In this way, cores of H50S subunits depleted of protein HmaL11 were obtained. The ribosomal subunits lacking protein HmaL11 crystallize under the same conditions as the native H50S subunits and at 10 Å show apparent isomorphism with them, indicating that the removal of this protein caused neither major conformational changes in the ribosome nor gross disturbances in the crystal's network. Therefore, it should be a suitable candidate for genetic insertions (Berkovitch-Yellin et al. 1992; Franceschi et al. 1993).

Surface characterization

An exact definition of the surface of the halophilic ribosomes is currently not possible because not all parameters influencing the ribosomal compactness have so far been identified. Nevertheless, several experiments focusing on the exposed regions of the rRNA and the r-proteins are being carried out.

Probing exposed single-stranded rRNA by complementary DNA oligomers

Recently, this procedure gained considerable popularity for mapping the ribosome surface (e.g., Weller and Hill 1991). Because the exposed rRNA regions, which are involved in functional activity, are rather conserved, several such regions have been located on halophilic and thermophilic ribosomes. DNA oligomers, targeting naturally exposed rRNA regions as well as those that become exposed by removing selected ribosomal proteins, have been synthesized. These may be used for derivatization because they can be prepared with a thiol group at their 5' end. The heavy atom clusters may be bound to this end (Franceschi et al. 1993).

The targeted regions include the last 14 nucleotides from the 3' end of the 16S RNA (the anti-"Shine-Dalgarno" regions) of T30S and three regions on H50S: bases 1125–1158 of the 23S RNA, homologous to those from *B. stearothermophilus*, which in the wild type are masked by protein BL11 but become exposed in the mutant lacking this protein; bases

1422–1432, the so-called "thiostrepton" binding site; and bases 2646–2667, the "alpha-sarcin" binding site (for review, see Sagi et al. 1995). Among the various undecabase oligomers, the tightest hybridization was obtained for the sequence 5'-AAGGAGGTGAT-3', used for complementing the anti-Shine-Dalgarno region of the 16S rRNA in T30S. Sucrose gradient centrifugation was performed to purify the hybrid from the unbound oligomers, and the hybridized particles were crystallized. In contrast, for the hybridization of the halophilic alpha-sarcin region, the salt concentration had to be lowered, suggesting that this site may not be exposed on the surface of the halophilic ribosomes.

Chemical probing of exposed ribosomal proteins

The surface ribosomal proteins are more manageable than the exposed rRNA; therefore, they are more suitable for the introduction of specific and quantitative modifications. Earlier accessibility studies were concentrated on limited proteolysis under conditions optimized for *E. coli* (Kruft and Wittmann-Liebold 1991). Attempts to extend the proteolytic experiments to the halophilic ribosomes were only partially successful because the halophilic ribosomes require high salinity for maintaining their compactness, whereas the conditions suitable for the proteolytic reaction of all commercially available enzymes are milder. Therefore, even when using the most robust proteolytic mixtures, partial unfolding of the halophilic ribosomes could have occurred. Such unfolding may not affect dramatically the overall sedimentation coefficient, showing that the gross integrity of the ribosomes is being kept, but at the same time, an opening-up of the compact active conformation and consequently exposing internal residues cannot be ruled out.

An alternative procedure is to decorate the surface of the ribosomes by chemical means. Our attempts at probing the exposed cysteines have been reported (Weinstein et al. 1989, 1992; Berkovitch-Yellin et al. 1992; Franceschi et al. 1993). The exposed amino groups, N-terminals and lysines' side chains, were probed by mild methylation, extending the procedures reported by Rayment et al. (1993) and by acylation with various radioactive agents. As expected, these modifications only reached completeness on a few occasions. In typical experiments, 30–60% of the lysines of H50S became modified, depending on the experimental conditions. It remains to be seen if the rest of the lysines are engaged in internal contacts. Interestingly, the H50S particles that were exposed to a rather low methylation levels (25% of the original amount) yielded crystals, which on several occasions reached an unusually large size (Sagi et al. 1995).

The modified proteins were detached from the particle and were digested with the endoprotease Lys-C from *isobacter* enzymogene, and the resulting peptides were analyzed for labeled lysines in their peptide maps. To date, several exposed regions have been identified on HmaL1 and HmaL12 (S. Weinstein and M. Peretz, unpublished).

H30S subunits behave differently and undergo substantial disintegration upon methylation, in accord with the lower stability and higher sensitivity found for several small eubacterial ribosomal subunits by different methods (Yonath and Wittmann 1989; Evers and Gewitz, 1989). In contrast, T30S was readily methylated to completion while maintaining its integrity.

Site-directed mutagenesis

The surface mapping experiments were synchronized with the characterization of the genes coding for the surface proteins that can be detached and reincorporated into core particles lacking them. Furthermore, these proteins were overproduced in *E. coli*, using the pET expression system (Studier et al. 1990). Despite the relatively low intracellular salt concentration of *E. coli*, the halophilic overexpressed proteins reached the level of 30–40% of the total cell proteins and remain soluble in the cytoplasm. Unexpected complications were encountered in attempts at cloning HmaL12 and the HmaL12/HmaL10 gene complex into the overexpression vectors, presumably because of unusual stable folding of this gene region. These were overcome by the design of the appropriate oligonucleotide primers according to the thermodynamic algorithm (Rychlik and Roads 1989).

As all overexpressed proteins can be incorporated into cores lacking them, giving rise to active ribosomal particles (Sagi et al. 1995), the way to site-directed mutagenesis became open. PCR (Picard et al. 1994) or the procedures described by Sayers et al. (1992) were used for site-directed mutagenesis. To date, 7 different mutants of HmaL1 and 10 of HmaL11 have been engineered and, in each case, a cysteine codon was inserted on different regions of the protein. To avoid undesired binding, the natural cysteine of HmaL11 was first blocked or exchanged because it was found to be unsuitable for labeling (see above and Franceschi et al. 1993).

The production of core particles, depleted of protein HmaL11 (see above), simplified the analysis of the incorporation of the mutated protein HmaL11. With the exception of two mutants, all could be incorporated into core particles. Screening for the suitability of the mutated proteins for binding heavy atom clusters is in progress. The differences in the ability of the various mutated proteins to incorporate into the depleted cores may provide indications about the conformation of the ribosomal proteins and (or) their specific in situ interactions. These are being currently analyzed.

The isolation and characterization of in situ complexes

The knowledge of the molecular structures of ribosomal components should provide a powerful tool for higher resolution structure determination of the entire particle. We anticipate to benefit from the crystallographic analysis of isolated r-proteins performed elsewhere, although it remains to be seen whether their structures reflect their in situ conformations. Internal small and defined substructures are more likely to maintain their native conformation because they may keep the in situ microenvironment. During the course of the surface mapping and depletion studies on H50S, we identified two in situ stable complexes. The first is between protein HmaL1 and a stretch of about 120 nucleotides of 23S rRNA, which was characterized mainly by limited digestion, the second is between the two proteins HmaL10 and HmaL12.

The experimental procedures and the biochemical properties of the ribonucleoprotein complex have been described (Evers et al. 1994). Interestingly, despite the "exotic" properties of the halophilic ribosomes and the evolutionary distance between *Haloarcula* and *E. coli*, both archaeobacterial components of this complex are readily interchangeable with their eubacterial counterparts (Evers et al. 1994).

The existence of a complex between proteins HmaL10 and

HmaL12 was revealed by the comparison of the two-dimensional gels of the total proteins of H50S and those belonging to the group detached by dioxane. It was shown that proteins HmaL10 and HmaL12 move together even at 8 M urea, indicating the existence of a stable complex between them. This complex dissociates into two separate proteins by dioxane and perhaps also in SDS. Although still not fully analyzed in quantitative terms, namely whether it contains one or four copies of protein L12, as found for eubacteria (reviewed in Moller and Maasen 1986), eukaryotes (Saenz-Robles et al. 1988), and other archaeobacteria (Casiano 1990), it is clear that this is a remarkably stable complex that does not disintegrate at 8 M urea or the FPLC conditions. Therefore, it is expected to form ordered crystals of a higher quality than those of its homolog from *B. stearothermophilus* (Liljas and Newcomer 1981).

Because all components of these complexes have been overexpressed, they are being produced in amounts sufficient for their crystallization as well as for their derivatization and incorporation in core particles. In addition, all three proteins participating in these complexes can be detached from H50S by dioxane, indicating that they are located at the surface of the particle, thus providing potential cluster binding sites. In case these complexes will yield high resolution structures, the combination of their structure with the expected localization of the clusters bound to them in the electron density map of the particle should be most important for further map interpretation.

Utilizing models reconstructed from crystalline monolayers for further studies

Images of the B70S ribosome and its large subunit from *B. stearothermophilus* were reconstructed at 47 and 28 Å, respectively, using tilt series of crystalline arrays, negatively stained with an inert material (Arad et al. 1987; Yonath et al. 1987). Although image reconstruction is not free from experimental and conceptual limitations, its superiority over conventional electron microscopy methods was demonstrated by the exclusive detection of several key features, associated mainly with internal vacant or partially filled hollows. Hence, despite their low resolution, the reconstructed models were provisionally interpreted (Yonath and Wittmann 1989). Consequently, it was suggested that the biosynthetic reaction occurs at the intersubunit interface, and plausible locations for the sheltered paths of the nascent proteins and of the mRNA chains were identified (Yonath and Wittmann 1989; Yonath and Berkovitch-Yellin 1993).

The reconstructed models inspired the design and the crystallization of complexes of ribosomal particles, mimicking defined functional states. These include B50S and H50S subunits to which one tRNA molecule and a short polypeptide are bound (Gewitz et al. 1988) and T70S ribosomes with a short stretch of mRNA and two molecules of tRNA (Hansen et al. 1990). The superiority of the latter over crystals of 70S ribosomes is evident. All three-dimensional crystals of 70S obtained to date are either too small or diffract to a very low resolution, 20–45 Å, presumably because of their significant conformational heterogeneity. In contrast, even the very simple complex, composed of T70S ribosome, two tRNA^{phe} molecules, and a chain of about 35 uridyl residues, led to a

dramatic improvement in the reproducibility of crystal growth and to an increase of over 10 Å in the resolution limits (Hansen et al. 1990).

More sophisticated complexes of T70S have recently been designed, aimed at increasing the homogeneity of the functional complexes of T70S and at minimizing the chances of protruding stretches of mRNA. These contain around 18 nucleotides, which is the approximate length of mRNA on both sides of the decoding site, which is masked by the ribosome (Beyer et al. 1994). Best results were obtained for (ATC)₅-CTT. Including in the reaction mixture charged tRNA^{ile} and omitting tRNA^{leu}, crystals of the complex with an average of 1.6 molecules of leu-tRNA^{ile} have been obtained.

Because tRNA participates in all complexes of ribosomal particles crystallized to date, trapped at defined functional states, a procedure was designed for the specific labeling of tRNA^{phe} and tRNA^{leu} by reagents, made of multimetal clusters, in a fashion that does not hamper the attachment of the corresponding amino acid and the binding to the ribosome (Weinstein et al. 1992). The complexes containing the gold-cluster-bound tRNA molecules were crystallized and are being exposed to crystallographic analysis.

The provisional interpretation of the reconstructed models stimulated various biochemical experiments, which in turn provided the basis for computed modelling in an attempt to shed light on the progression of the growing polypeptide chains (Eisenstein et al. 1994; Hardesty et al. 1995). Of particular interest is the fate of the MS2 coat protein. Biochemical studies indicated that the labeled N-terminal of this protein is not available for interaction with antibodies raised against the label until the protein reaches its full length, 129 amino acid residues. Indeed, the modelling experiments showed that the entire protein can be accommodated in a partially folded conformation within the tunnel that spans the 50S subunit, assumed to be the path of the nascent chains. These findings are in accord with results of activation-release studies showing that the final steps in the folding of nascent proteins are mediated by chaperons associated with the ribosome (Kudlicki et al. 1994a, 1994b; Eisenstein et al. 1994; Hardesty et al. 1995).

It is clear that a higher resolution is essential for more accurate assignments; therefore, image reconstruction experiments from unstained crystalline arrays in vitrified ice are being carried out. Preliminary efforts led to the growth of arrays of B50S subunits, diffracting to about 15 Å resolution (Avila-Sakar et al. 1994).

Conclusions and prospects

From the early stages of ribosomal crystallography, it was clear that a straightforward application of conventional concepts and techniques of macromolecular crystallography would not be adequate. Hence, we designed an approach that combines the exploitation of the extensive information available on the genetic, functional, and chemical properties of ribosomes for a rational design of protocols for crystallization and for derivatization with dense clusters or multiatom salts. As seen, preliminary maps at intermediate resolution, which show features of the size expected for the corresponding ribosomal particles, have already been constructed. Furthermore, since the native and several derivatized crystals diffract to relatively high resolution, up to 2.9 Å for H50S and 7.3 Å for

T30S, a more detailed map is anticipated in the foreseeable future.

Acknowledgements

The studies presented here have been initiated under the inspiration and guidance of the late Prof. H.G. Wittmann. We are grateful for the excellent experimental assistance provided by Mr. K. Knaack and T. Arad as well as Ms. C. Glotz, R. Albrecht, C. Paulke, J. Müssig, J. Piefke, R. Hasenbank, B. Romberg, I. Dunkel, B. Schroeter, S. Meyer, C. Radzwill, B. Donzelmann, M. Laschever, and P. Baruch. We thank Drs. M. Pope, W. Jahn, R. Huber, W. Bode, and W. Preetz for their gifts of multimetal compounds and Dr. F. Triana for the preparation of tRNA molecules. We also thank Drs. M. Roth, E. Pebay-Peyroula, B. Hardesty, T. Choli, A. Podjarny, W. Hill, E. Dabbs, K.R. Leonard, and W. Chiu for their active participation in the studies presented here and for their illuminating comments. Experiments were carried out at the Weizmann Institute in Israel, the Max-Planck Research Unit in Hamburg, and the Max-Planck Institute for Molecular Genetics in Berlin. Data were collected with synchrotron beam as follows: EMBL and MPG lines at DESY; F1 at CHESS, Cornell U.; SSRL, Stanford U.; PF/KEK, Japan. Support was provided by the National Institutes of Health (NIH GM 34360), the German Space Agency (DARA, 50QV 86061), the Minerva Fellowship Program, and the Kimmelman Center for Macromolecular Assembly at Weizmann Institute. A.Y. holds the Martin S. Kimmel Professorial Chair.

References

- Alizadeh, M.H., Harmalker, S.P., Jeannin, Y., Martin-Frere, J., and Pope, M.T. 1985. A heteropolyanion with fivefold molecular symmetry that contains a nonlabile encapsulated sodium ion. The structure and chemistry (NaP₅W₃₀O₁₁₀)¹⁴⁻. *J. Am. Chem. Soc.* **107**: 2662–2669.
- Arad, T., Piefke, J., Weinstein, S., Gewitz, H.S., Yonath, A., and Wittmann, H.G. 1987. Three-dimensional image reconstruction from ordered arrays of 70S ribosomes. *Biochimie*, **69**: 1001–1006.
- Avila-Sakar, A.J., Guan, T.L., Schmid, M.F., Loke, T.L., Arad, T., Yonath, A., Piefke, J., Franceschi, F., and Chiu, W. 1994. Electron cryomicroscopy of *B. stearothermophilus* 50S ribosomal subunits crystallized on phospholipid monolayer. *J. Mol. Biol.* **239**: 689–697.
- Bartels, H., Bennett, W.S., Hansen, H.A.S., Eisenstein, M., Weinstein, S., Müssig, J., Volkmann, N., Schlünzen, F., Agmon, I., Franceschi, F., and Yonath, A. 1995. The suitability of a mono functional reagent of an undecagold cluster for phasing data collected from the large ribosomal subunit from *Bacillus stearothermophilus*. *Biopolymers (Peptide Science)*, **37**: 411–419.
- Berkovitch-Yellin, Z., Bennett, W.S., and Yonath, A., 1992. Aspects in structural studies on ribosomes. *Crit. Rev. Biochem. Mol. Biol.* **27**: 403–439.
- Berkovitch-Yellin, Z., Wittmann, H.G., and Yonath, A. 1990. Low resolution models for ribosomal particles reconstructed from electron micrographs of tilted two-dimensional sheets: tentative assignments of functional sites. *Acta Cryst. B*, **46**: 637–42.
- Beyer, D., Skripkin, E., Wadzack, J., and Nierhaus, K.H. 1994. How the ribosome moves along the mRNA during protein synthesis. *J. Biol. Chem.* **269**(48): 30 713 – 30 717.
- von Böhlen, K., Makowski, I., Hansen, H.A.S., Bartels, H., Berkovitch-Yellin, Z., Zaytzev-Bashan, A., Meyer, S., Paulke, C.,

- Franceschi, F., and Yonath, A. 1991. Characterization and preliminary attempts for derivatization of crystals of large ribosomal subunits from *Haloarcula marismortui*, diffracting to 3 Å resolution. *J. Mol. Biol.* **222**: 11–15.
- Bricogne, G. 1984. Maximum entropy and the foundation of direct methods. *Acta Cryst. A*, **40**: 410–445.
- Brown, G.M., Noe Spirlet, M.R., Busig, W.R., and Levy, H.A. 1977. Dodecatungstophosphoric acid hexahydrate (H_5O_2^+)₃($\text{PO}_{12}\text{O}_{40}^{-3}$). The true structure of Keggin's pentahydrate for single crystal X-ray and neutron diffraction. *Acta Cryst. B*, **33**: 1038–1046.
- Casiano, C., Matheson, A.T., and Traut, R.R. 1990. Occurrence in archaeobacterium *Sulfolobus solfataricus* of a ribosomal protein complex corresponding to *E. coli* (L7/L12)₄L10 and eukaryotic (P1)₂/(P2)₂. *PO. J. Biol. Chem.* **265**: 18 757–18 761.
- Dawson, B. 1953. The structure of the 9(18) heteropoly anion in potassium 9(18) tungstophosphate, $\text{K}_6(\text{P}_2\text{W}_{15}\text{O}_{62})14\text{H}_2\text{O}$. *Acta Cryst.* **6**: 113–118.
- Eisenstein, M., Sharon, R., Berkovitch-Yellin, Z., Gewitz, H.S., Weinstein, S., Pebay-Peyroula, E., Roth, M., and Yonath, A. 1991. The interplay between X-ray crystallography, neutron diffraction, image reconstruction, organo-metallic chemistry, and biochemistry in structural studies of ribosomes. *Biochimie*, **73**: 879–886.
- Eisenstein, M., Hardesty, B., Odom, M., Kudlicki, W., Kramer, G., Arad, T., Franceschi, F., and Yonath, A. 1994. Modelling the experimental progression of nascent protein in ribosomes. *In* Supramolecular structure. *Edited by* G. Pifat. Balaban Press, Rehovot. pp. 213–246.
- Evers, U., and Gewitz, H.S. 1989. Studied on the accessibility of nascent non-helical peptide chains on the ribosome. *Biochem. Int.* **19**: 1031–1038.
- Evers, U., Franceschi, F., Boeddeker N., and Yonath, A. 1994. Crystallography of halophilic ribosomes: the isolation of an internal ribonucleoprotein complex. *Biophys. Chem.* **50**: 3–16.
- Franceschi, F., Weinstein, S., Evers, U., Arndt, E., Jahn, W., Hansen, H.A.S., von Böhlen, K., Berkovitch-Yellin, Z., Eisenstein, M., Agmon, I., Thygesen, J., Volkmann, N., Bartels, H., Schlünzen, F., Zaytzev-Bashan, A., Sharon, R., Levin, I., Dribin, A., Sagi, I., Choli-Papadopoulou, T., Tsiboli, P., Kryger, G., Bennett, W.S., and Yonath, A. 1993. Towards atomic resolution of prokaryotic ribosomes: crystallographic, genetic and biochemical studies. *In* The translational apparatus. *Edited by* K. Nierhaus. Plenum Press, New York. pp. 397–410.
- Franceschi, F., Sagi, I., Bödder, N., Evers, U., Arndt, E., Paulke, C., Hasenbank, R., Laschever, M., Glotz, C., Piefke, J., Müssig, J., Weinstein, S., and Yonath, A. 1994. Crystallography, biochemical and genetics studies on halophilic ribosomes. *In* Molecular biology of archaea. *Edited by* F. Pfeifer, P. Palm, and K.H. Schleifer. Gustav Fischer Verlag, Stuttgart, Germany. pp. 197–205.
- Franceschi, F., Weinstein, S., Sagi, I., Peretz, M., Weinrich, V., Morlang, S., Boeddeker, N., Geva, M., Levin, I., Agmon, I., Berkovitch-Yellin, Z., Schlunzen, F., Hansen, H.A.S., Bartels, H., Bennett, W.S., Volkmann, N., Thygesen, J., Harms, J., Zaytzev-Bashan, A., Krumbholz, S., Sharon, R., Dribin, A., Maltz, E., and Yonath, A. 1996. The combination of functional, genetics, microscopical and crystallographical studies led to initial phasing of data collected from ribosomal crystals at intermediate resolution. *In* The ninth conversation in biomolecular stereodynamics. *Edited by* R. Sarma. In press.
- Gewitz, H.S., Glotz, C., Piefke, J., Yonath, A., and Wittmann, H.G. 1988. Two-dimensional crystalline sheets of the large ribosomal subunits containing the nascent protein chain. *Biochimie*, **70**: 645–648.
- Giacovazzo, C. 1980. Direct methods in crystallography. Academic Press, London.
- Hansen, H.A.S., Volkmann, N., Piefke, J., Glotz, C., Weinstein, S., Makowski, I., Meyer, S., Wittmann H.G., and Yonath, A. 1990. Crystals of complexes mimicking protein biosynthesis are suitable for crystallographic studies. *Biochim. Biophys. Acta*, **1050**: 1–5.
- Hardesty, B., Yonath, A., Kramer, G., Odom, O.W., Eisenstein, M., Franceschi, F., and Kudlicki, W. 1995. The conformation and path of nascent proteins in ribosomes. *In* Membrane protein transport. Vol. 1. *Edited by* S.S. Rothman. pp. 77–107.
- Jahn, W. 1989a. Synthesis of water soluble undecagold cluster for specific labeling of proteins. *Z. Naturforsch. Sect. B, Chem. Sci.* **44**: 1313–1316.
- Jahn, W. 1989b. Synthesis of water soluble tetrairidium clusters suitable for heavy atom labeling of proteins. *Z. Naturforsch. Sect. B, Chem. Sci.* **44**: 79–82.
- Kruft, V., and Wittmann-Liebold, B. 1991. Determination of peptide regions on the surface of the eubacterial and archaeobacterial ribosome by limited proteolytic digestion. *Biochemistry*, **30**: 11 781–11 787.
- Kudlicki, W., Odom, O.W., Kramer, G., and Hardesty, B. 1994a. Activation and release of enzymatically inactive, full-length rhodanese that is bound to ribosomes as peptidyl-tRNA. *J. Biol. Chem.* **269**: 16 549–16 553.
- Kudlicki, W., Odom, O.W., Kramer, G., and Hardesty, B. 1994b. Chaperone-dependent folding and activation of ribosome bound rhodanese. Analysis by fluorescence. *J. Mol. Biol.* **244**: 319–331.
- Liljas, A., and Newcomer, M.E. 1981. Purification and crystallization of protein complex from *Bacillus stearothermophilus*. *J. Mol. Biol.* **153**: 393–398.
- Löwe, J., Stock, D., Jap, B., Zwickl, P., Baumeister, W., and Huber, R. 1995. Crystal structure of the 20S proteasome from the Archaeon *T. acidophilum* at 3.4 Å resolution. *Science (Washington, D.C.)*, **268**: 533–539.
- Lunin, V.Y., Lunina, N.M., Petrova, T.E., Vernoslava, E.A., Urzhumstev, A.G., and Podjarny, A.D. 1995. On the ab initio solution of the phase problem at very low resolution: the few atom method. *Acta Cryst. D*, **51**: 896–903.
- Moller, W., and Maasen, J.A. 1986. On the structure, function and dynamics of L7/L12 from *E. coli* ribosomes. *In* Structure, function and genetics of ribosomes. *Edited by* B. Hardesty and G. Kramer. Springer Verlag, New York. pp. 309–325.
- Müssig, J., Makowski, I., von Böhlen, K., Hansen, H., Bartels, K.S., Wittmann, H.G., and Yonath, A. 1989. Crystals of wild-type, mutated, derivatized and complexed 50S ribosomal subunits from *Bacillus stearothermophilus* suitable for X-ray analysis. *J. Mol. Biol.* **205**: 619–622.
- Picard, V., Edsal-Badju, E., Lu, A., and Book, S.C. 1994. A rapid efficient one-tube PCR-based mutagenesis technique using Pfu DNA polymerase. *Nucleic Acids Res.* **22**: 2587–2591.
- Rayment, I., Wojciech, R., Rypniewski, W.R., Schmidt-Base, K., Smith, R., Tomchick, D.R., Benning, M.M., Winkelmann, D.A., Wesenberg, G., and Holden, H.M. 1993. Three-dimensional structure of myosin subfragment-1: a molecular motor. *Science (Washington, D.C.)*, **261**: 50–53.
- Roth, M., and Pebay-Peyroula, E. 1995. Low resolution ab initio phasing using direct methods. *In* Entropy, likelihood, Bayesian inference and their application in crystal structure determination. *Edited by* G. Bricogne. Am. Cryst. Assoc., Buffalo, N.Y. In press.
- Rychlik, W., and Rhoads, R. 1989. A computer program for choosing optimal oligonucleotides for filter hybridization, sequencing and in vitro amplification of DNA. *Nucleic Acid Res.* **17**: 8543–8551.
- Saenz-Robles, M.T., Vilella, M.D., Pucciarelli, G., Polo, F., Remacha, M., Ortiz, B.L., Vidales, F.J., and Ballesta, J.P.G. 1988. Ribosomal proteins interactions in yeast: protein L15 forms a complex with the acidic proteins. *Eur. J. Biochem.* **177**: 531–537.

- Sagi, I., Weinrich, V., Levin, I., Glotz, C., Laschever, M., Melamud, M., Franceschi, F., Weinstein, S., and Yonath, A. 1995. Crystallography of ribosomes: attempts at decorating the ribosomal surface. *Biophys. Chem.* **55**: 31–41.
- Schneider, G., and Lindquist, Y. 1994. Ta₆Br₁₄ is a useful cluster compound for isomorphous replacement in protein crystallography. *Acta Cryst. D*, **50**: 186–191.
- Schlünzen, F. 1994. Crystallographic investigations on the 50S ribosomal subunits from *Thermus thermophilus*. Ph.D. thesis, University of Hamburg, Germany.
- Studier, F.W., Rosenberg, A.H., Dunn, J.J., and Dubendorf, J.W. 1990. Use of T7 polymerase to direct expression of cloned genes. *Methods Enzymol.* **185**: 60–88.
- Sayers, J.R., Krekel, C., and Eckstein, F. 1992. Rapid high-efficiency site directed mutagenesis by the phosphothioate approach. *Biotechniques*, **13**: 592–596.
- Tsiboli, P., Herfurth, E., and Choli, T. 1994. Purification and characterization of the 30S ribosomal proteins from the bacterium *Thermus thermophilus*. *Eur. J. Biochem.* **226**(1): 169–177.
- Urzhumstev, A.G., and Podjarny, A.D. 1995. On the solution of the molecular replacement problem at very low resolution. *Acta Cryst. D*, **51**: 888–895.
- Volkman, N. 1993. Maximum entropy and the phase problem for ribosomal crystallography. Ph.D. thesis, University of Hamburg, Germany.
- Volkman, N. 1995. Maximum entropy, likelihood, and the large ribosomal subunit from *Thermus thermophilus*. In *Entropy, likelihood, Bayesian inference and their application in crystal structure determination*. Edited by G. Bricogne. Am. Cryst. Assoc., Buffalo, N.Y. In press.
- Volkman, N., Schlünzen, F., Vernoslava, E.A., Urzhumstev, A.G., Podjarny, A.D., Roth M., Pebay-Peyroula, E., Berkovitch-Yellin, Z., Zaytzev-Bashan, A., and Yonath, A. 1995. On low-resolution non-MIR phasing of ribosomal particles. Joint CCP4 and ESF-EACBM Newsletters, June 95. pp. 25–28.
- Weinstein, S., Jahn, W., Wittmann, H.G., and Yonath, A. 1989. Novel procedures of derivatization of ribosomes for crystallographic studies. *J. Biol. Chem.* **264**: 19 138 – 19 142.
- Weinstein, S., Jahn, W., Laschever, M., Arad, T., Tichelaar, W., Haider, M., Glotz, C., Boeckh, T., Berkovitch-Yellin, Z., Franceschi, F., and Yonath, A. 1992. Derivatization of ribosomes and of tRNA with an undecagold cluster: crystallographic and functional studies. *J. Cryst. Growth*, **122**: 286–292.
- Weller, J., and Hill, W.E. 1991. Probing the initiation complex formation on *E. coli* ribosomes using short complementary DNA oligomers. *Biochimie*, **73**: 971–981.
- Wittmann-Liebold, B., Koepke, A., Arndt, E., Kroemer, W., Hatakayama, T., and Wittmann, H.G. 1990. Sequence comparison and evolution of ribosomal proteins and their genes. In *The ribosomes: structure, function, and evolution*. Edited by E.W. Hill, A. Dahlbert, R.A. Garrett, P.B. Moore, D. Schlessinger, and J.R. Warner. Am. Soc. Microbiol., Washington, D.C. pp. 598–616.
- Yonath, A., Leonard, K.R., and Wittmann, H.G. 1987. A tunnel in the large ribosomal subunit revealed by three-dimensional image reconstruction. *Science* (Washington, D.C.), **236**: 813–817.
- Yonath, A., Glotz, C., Gewitz, H.S., Bartels, K., von Böhlen, K., Makowski, I., and Wittmann, H.G. 1988. Characterization of crystals of small ribosomal subunits. *J. Mol. Biol.* **203**: 831–834.
- Yonath, A., and Wittmann, H.G. 1989. Challenging the three-dimensional structure of ribosomes. *TIBS*, **14**: 329–334.
- Yonath, A., and Berkovitch-Yellin, Z. 1993. Hollows, voids, gaps and tunnels in the ribosome. *Curr. Opin. Struct. Biol.* **3**: 175–181.
- Zaytzev-Bashan, A. 1995. Crystallographic studies on the large ribosomal subunits from halophilic and thermophilic bacteria. Ph.D. thesis, Weizmann Institute, Rehovot, Israel.

This article has been cited by:

1. Thomas D. Grant, Joseph R. Luft, Jennifer R. Wolfley, Hiro Tsuruta, Anne Martel, Gaetano T. Montelione, Edward H. Snell. 2011. Small angle X-ray scattering as a complementary tool for high-throughput structural studies. *Biopolymers* **95**:10.1002/bip.v95.8, 517-530. [[CrossRef](#)]
2. Thomas A. Steitz. 2010. From the Structure and Function of the Ribosome to New Antibiotics (Nobel Lecture). *Angewandte Chemie International Edition* **49**, 4381-4398. [[CrossRef](#)]
3. Thomas A. Steitz. 2010. Von der Struktur und Funktion des Ribosoms zu neuen Antibiotika (Nobel-Aufsatz). *Angewandte Chemie* **122**, 4482-4500. [[CrossRef](#)]
4. Peter B. Moore, Thomas A. Steitz. 2003. THE STRUCTURAL BASIS OF LARGE RIBOSOMAL SUBUNIT FUNCTION. *Annual Review of Biochemistry* **72**, 813-850. [[CrossRef](#)]
5. William M. Clemons, Ditlev E. Brodersen, John P. McCutcheon, Joanna L.C. May, Andrew P. Carter, Robert J. Morgan-Warren, Brian T. Wimberly, V. Ramakrishnan. 2001. Crystal structure of the 30 S ribosomal subunit from *Thermus thermophilus*: purification, crystallization and structure determination. *Journal of Molecular Biology* **310**, 827-843. [[CrossRef](#)]
6. D.E. BRODERSEN, A.P. CARTER, W.M. CLEMONS, R.J. MORGAN-WARREN, F.V. MURPHY, J.M. OGLE, M.J. TARRY, B.T. WIMBERLY, V. RAMAKRISHNAN. 2001. Atomic Structures of the 30S Subunit and Its Complexes with Ligands and Antibiotics. *Cold Spring Harbor Symposia on Quantitative Biology* **66**, 17-32. [[CrossRef](#)]
7. J.L. HANSEN, T.M. SCHMEING, D.J. KLEIN, J.A. IPPOLITO, N. BAN, P. NISSEN, B. FREEBORN, P.B. MOORE, T.A. STEITZ. 2001. Progress Toward an Understanding of the Structure and Enzymatic Mechanism of the Large Ribosomal Subunit. *Cold Spring Harbor Symposia on Quantitative Biology* **66**, 33-42. [[CrossRef](#)]
8. Shulamith Weinstein, Werner Jahn, Carola Glotz, Frank Schlünzen, Inna Levin, Daniela Janell, Jörg Harms, Ingo Kölln, Harly A.S. Hansen, Marco Glühmann, William S. Bennett, Heike Bartels, Anat Bashan, Ilana Agmon, Maggie Kessler, Marta Pioletti, Horacio Avila, Kostas Anagnostopoulos, Moshe Peretz, Tamar Auerbach, Francois Franceschi, Ada Yonath. 1999. Metal Compounds as Tools for the Construction and the Interpretation of Medium-Resolution Maps of Ribosomal Particles. *Journal of Structural Biology* **127**, 141-151. [[CrossRef](#)]
9. Jörg Harms, Ante Tocilj, Inna Levin, Ilana Agmon, Holger Stark, Ingo Kölln, Marin van Heel, Marianne Cuff, Frank Schlünzen, Anat Bashan, Francois Franceschi, Ada Yonath. 1999. Elucidating the medium-resolution structure of ribosomal particles: an interplay between electron cryo-microscopy and X-ray crystallography. *Structure* **7**, 931-941. [[CrossRef](#)]
10. D. R. Benjamin, C. V. Robinson, J. P. Hendrick, F. U. Hartl, C. M. Dobson. 1998. Mass spectrometry of ribosomes and ribosomal subunits. *Proceedings of the National Academy of Sciences* **95**, 7391-7395. [[CrossRef](#)]
11. Peter B. Moore. 1998. THE THREE-DIMENSIONAL STRUCTURE OF THE RIBOSOME AND ITS COMPONENTS. *Annual Review of Biophysics and Biomolecular Structure* **27**, 35-58. [[CrossRef](#)]
12. Nenad Ban, Betty Freeborn, Poul Nissen, Pawel Penczek, Robert A. Grassucci, Robert Sweet, Joachim Frank, Peter B. Moore, Thomas A. Steitz. 1998. A 9 Å Resolution X-Ray Crystallographic Map of the Large Ribosomal Subunit. *Cell* **93**, 1105-1115. [[CrossRef](#)]
13. Anders Liljas, Salam Al-Karadaghi. 1997. Structural aspects of protein synthesis. *Nature Structural Biology* **4**, 767-771. [[CrossRef](#)]
14. D.I Svergun, N Burkhardt, J.Skov Pedersen, M.H.J Koch, V.V Volkov, M.B Kozin, W Meerwink, H.B Stuhmann, G Diedrich, K.H Nierhaus. 1997. Solution scattering structural analysis of the 70 S *Escherichia coli* ribosome by contrast variation. I. invariants and validation of electron microscopy models. *Journal of Molecular Biology* **271**, 588-601. [[CrossRef](#)]
15. Peter B Moore. 1997. The conformation of ribosomes and rRNA. *Current Opinion in Structural Biology* **7**, 343-347. [[CrossRef](#)]
16. Rachel Green and, Harry F. Noller. 1997. RIBOSOMES AND TRANSLATION. *Annual Review of Biochemistry* **66**, 679-716. [[CrossRef](#)]
17. Ada Yonath, Francois Franceschi. 1997. New RNA recognition features revealed in ancient ribosomal proteins. *Nature Structural Biology* **4**, 3-5. [[CrossRef](#)]
18. Knud H. Nierhaus, Heinrich B. Stuhmann, Dmitri Svergun The Ribosomal Elongation Cycle and the Movement of tRNAs across the Ribosome 177-204. [[CrossRef](#)]
19. J. Thygesen, S. Krumbholz, I. Levin, A. Zaytzev-Bashan, J. Harms, H. Bartels, F. Schlünzen, H.A.S. Hansen, W.S. Bennett, N. Volkmann, I. Agmon, M. Eisenstein, A. Dribin, E. Maltz, I. Sagi, S. Morlang, M. Fua, F. Franceschi, S. Weinstein, N. Bøddeker, R. Sharon, K. Anagnostopoulos, M. Peretz, M. Geva, Z. Berkovitch-Yellin, A. Yonath. 1996. Ribosomal crystallography: from crystal growth to initial phasing. *Journal of Crystal Growth* **168**, 308-323. [[CrossRef](#)]